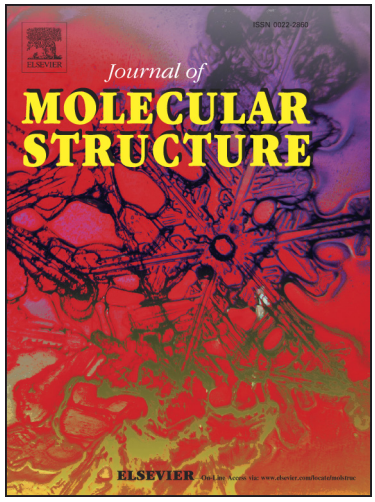

Triquinane scaffolds: Shape and geometry as a function of saturation and bridgehead groups

Lois-May Young, Matthias Zeller, Werner J. Geldenhuys, Sarel F. Malan, Cornelis J. Van der Schyf

PII: S0022-2860(13)00326-8
DOI: http://dx.doi.org/10.1016/j.molstruc.2013.04.030
Reference: MOLSTR 19685

To appear in: *Journal of Molecular Structure*

Received Date: 27 November 2012
Revised Date: 12 April 2013
Accepted Date: 12 April 2013

Please cite this article as: L-M. Young, M. Zeller, W.J. Geldenhuys, S.F. Malan, C.J. Van der Schyf, Triquinane scaffolds: Shape and geometry as a function of saturation and bridgehead groups, *Journal of Molecular Structure* (2013), doi: http://dx.doi.org/10.1016/j.molstruc.2013.04.030

Triquinane scaffolds: Shape and geometry as a function of saturation and bridgehead groups.

Lois-May Young,[a] Matthias Zeller,[b] Werner J. Geldenhuys,[c] Sarel F. Malan,[d] and Cornelis J. Van der Schyf[a,c*]

[a]Pharmaceutical Chemistry, School of Pharmacy, North-West University, Potchefstroom 2520, South Africa, [b]Department of Chemistry, Youngstown State University, Youngstown, Ohio 44555, USA, [c]Department of Pharmaceutical Sciences, Northeast Ohio Medical University, Rootstown, Ohio 44272, USA, [d]School of Pharmacy, University of the Western Cape, Bellville, 7535, South Africa

*To whom correspondence should be addressed. Lois-May Young, Address: (present address) 5/10 Victoria Parade, Manly, NSW 2095, Australia. E-mail: y.loismay@gmail.com, phone: +61-416-358-280 and Cornelis J. Van der Schyf: Address, Northeast Ohio Medical University, 4209 State Route 44, Rootstown, OH 44272; E-mail, cvanders@neomed.edu, phone, +1-330-325-6467.

Abstract

Polycyclic hydrocarbon compounds, also known as "cage compounds", are of interest in drug discovery due to their versatility as scaffolds. Derivatives of both pentacycloundecane-dione and triquinane-dione have been the focus of numerous investigations as multifunctional neuroprotective drugs where these compounds were used as novel drug scaffolds with the ability to cross the blood brain barrier. Here we present the synthesis, characterization and single crystal X-ray analysis for two triquinane synthons; tricyclo[6.3.0.$0^{2,6}$]undecane-4,9-diene-3,11-dione (compound **5** crystallizes in the monoclinic system, unit cell parameters are: a = 6.5876 (12) Å, b = 10.4204 (19) Å, c = 12.074 (2) Å; V = 825.4 (3) $Å^3$ and Z = 4) and tricyclo[6.3.0.$0^{2,6}$]undecane-3,11-dione (compound **6** crystallizes in monoclinic system, unit cell parameters are: a = 7.5992 (7) Å, b = 10.7294 (10) Å, c = 10.8664 (10) Å; V = 884.04 (14) $Å^3$ and Z = 4); as well as a triquinane derivative, *N*-(3-methoxybenzyl)-3,11-azatricyclo[6.3.0.$0^{2,6}$]undecane (compound **11** crystallizes in triclinic system, unit cell parameters are: a = 7.6714 (7) Å, b = 9.0100 (9) Å, c = 11.2539 (11) Å; V = 745.78 (12) $Å^3$ and Z = 2). The size and geometrical conformation of the triquinane scaffolds were compared to tetra and pentacycloundecanes, revealing that tricyclo[6.3.0.$0^{2,6}$]undecane-3,11-dione experiences strain relieve resulting in greater flexibility, a more asymmetric molecular shape and larger surface are. However, with the introduction of the aza-bridge in *N*-(3-methoxybenzyl)-3,11-azatricyclo[6.3.0.$0^{2,6}$]undecane, much of the flexibility and asymmetry is lost again. We also discuss the rearrangement mechanism for the observed retro cycloaddition and reversion, and utilized density functional theory calculations to discuss the photocyclization mechanism of this unique [2+2] Diels-Alder system.

Keywords: Polycyclic cage, pentacycloundecane, triquinane, crystal structure, L-type calcium channel blockers.

1. Introduction

Pentacyclo[5.4.0.0^{2,6}.0^{3,10}.0^{5,9}]undecane-8,11-dione (PCU, **4**, scheme 1) is of interest in drug discovery because of its unique cage-like structure that serves as a lipophilic scaffold for synthesizing drugs with neuroprotective properties and the ability to cross the blood brain barrier [1]. The polycyclic scaffold also has the ability to modify and improve pharmacokinetic and pharmacodynamic properties of drugs [2, 3]. A well-known example of such a derivative is 8-benzylamino-8,11-oxopentacyclo[5.4.0.0^{2,6}.0^{3,10}.0^{5,9}]undecane (NGP1-01), widely reported for its activity as a multifunctional neuroprotective drug (reviewed in [4]). NGP1-01 has been shown to be a L-type calcium channel blocker in both neuronal and heart cells [5, 6], and also acts – in a dual mechanistic way – as an *N*-methyl-D-aspartate (NMDA) receptor antagonist [7, 8]. PCU (**4**) is also utilized as an intermediate in the synthesis of polyquinane natural products [9], of which tricyclo[6.3.0.0^{2,6}]undecane-4,9-diene-3,11-dione (**5**) and tricyclo[6.3.0.0^{2,6}]undecane-3,11-dione (**6**) and their derivatives are of particular interest to our group. The triquinane scaffold was first synthesized by our group to test the validity of the hypothesis that the pentacycloundecane skeleton serve only as a bulk contributor to the biological activity of the polycyclic cage and its derivatives [10].

The triquinane scaffold and triquinylamine derivatives can be obtained *via* thermal fragmentation of PCU and subsequent catalytic reduction [10]. These derivatives

showed suppression of the calcium action potential (AP) in guinea-pig papillary muscle [10]. Aromatic triquinylamine derivatives were capable of completely suppressing the AP while aliphatic derivatives suppressed the AP by ~ 50%. These compounds were also able to significantly slow heart rate. It was concluded that ring opening of the cage moiety did not diminish the calcium channel blocking activity, or the negative chronotropic effects of these types of compounds [10]. These findings reiterated that the triquinane system may afford a useful and novel synthon, and together with appropriate side chain derivatization, it can be utilized to develop multifunctional compounds that can be of use in the treatment of neurodegenerative diseases. The concept of utilizing L-type calcium channel blockers in the treatment of neurodegenerative diseases has also been explored by other authors [11, 12]. This study forms part of an extensive study in which we utilized several pentacycloundecane and triquinane derivatives to determine their IC_{50} values as L-type calcium channel blockers. Here we report the synthesis and X-ray crystal structure investigations of the two scaffolds; tricyclo[6.3.0.$0^{2,6}$]undecane-4,9-diene-3,11-dione (**5**) and tricyclo[6.3.0.$0^{2,6}$]undecane-3,11-dione (**6**) as well as a substituted derivative, *N*-(3-methoxybenzyl)-3,11-azatricyclo[6.3.0.$0^{2,6}$]undecane (**11**). This derivative (**11**) showed promising potential as an L-type calcium channel blocker in a QSAR study (data to be published). Additionally, we elaborate on the reaction mechanism of the cycloreversion of (**4**) and the retro cycloaddition of (**5**) utilizing molecular modeling.

2. Experimental

2.1. Synthesis

Pentacyclo[5.4.0.0^{2,6}.0^{3,10}.0^{5,9}]undecane-8,11-dione (**4**) was synthesized as previously described (Scheme 3) [13], and the crystal structure for this compound has also been reported [13, 14]. Tricyclo[6.3.0.0^{2,6}]undecane-4,9-diene-3,11-dione (**5**) can be obtained through thermal fragmentation (Scheme 1), by means of flash vacuum pyrolysis of the saturated four-membered ring (**4**) [9]. The melting point of (**5**) was determined by DSC to be 97.23 ºC. Catalytical hydrogenation of the thermolysis product (**5**) yielded tricyclo[6.3.0.0^{2,6}]undecane-3,11-dione (**6**) [10]. The melting point of this compound was determined by DSC to be 95.82 ºC. We have also encountered the reversible nature of the cycloreversion [15] that yielded the *cis-syn-cis* linearly fused triquinane system (Scheme 3), in our attempts to polymerize (**5**) *via* a radical mechanism utilizing ultra violet (UV) irradiation through a 450W UV lamp (quartz, EtOAc).

To obtain *N*-(3-methoxybenzyl)-3,11-azatricyclo[6.3.0.0^{2,6}]undecane (**11**) (Scheme 2), tricyclo[6.3.0.0^{2,6}]undecane-3,11-dione (**6**) (3.01 g, 0.0169 mol) was dissolved in anhydrous THF (30 ml), stirred and cooled to 5 °C on an external ice bath. An equimolar quantity of 3-methoxybenzylamine (2.32 g, 0.0169 mol) was slowly added, while the mixture was stirred for approximately 6 h at reduced temperature. Upon completion the solvent was removed *in vacuo* to yield the carbonylamine (**9**) as an oil. This product was dehydrated under Dean Stark conditions for approximately 1 h using 40 ml anhydrous benzene. The benzene was removed *in vacuo* to afford Schiff base **10**. The resulting oil was dissolved in anhydrous MeOH (20 ml) and anhydrous THF (75 ml). Reduction was carried out by the addition of $NaBH_3CN$ in one molar excess and stirring

overnight (18 h) at room temperature. The solvent was removed *in vacuo* to yield the final product (**11**) as a dark colored oil. This oil was suspended in approximately 50 ml of distilled water in a separation funnel. The product was extracted with DCM (4 × 20 ml) and the combined DCM fractions were washed with distilled water (2 × 50 ml). The organic phase was dried over anhydrous $CaSO_4$ and filtered. The solvent was removed *in vacuo*. The compound was purified using a two-step silica column chromatography approach. The first purification step utilized PE:$CHCl_3$:EtOAc, 10:6:1 as the eluant mixture, and the second PE:THF, 5:1 at a lower temperature (5 °C). Purification afforded a light yellow oil (yield: 0.4523 g, 0.002 mol, 9.46 %). From this oil the compound was crystallized in EtOAc to obtain colorless crystals suitable for X-ray crystallographic analysis.

2.2. NMR spectroscopy

^{1}H-NMR and ^{13}C-NMR spectra were obtained using a Varian Gemini 300 spectrometer at a frequency of 300.075 MHz and 75.462 MHz, respectively. This was done in a 7 Tesla magnetic field and tetramethylsilane (TMS) was used as internal standard. A bandwidth of 1,000 MHz at 24 kG was applied for ^{1}H-^{13}C-decoupling. All chemical shifts are reported in parts per million (ppm) relative to the signal of TMS ($\delta = 0$) added to the deuterated solvent, $CDCl_3$. Distorsionless Enhancement by Polarisation Transfer (DEPT) experiments were also conducted for these compounds.

2.3. X-ray Crystallography Analysis

Diffraction data for (**5**), (**6**) and (**11**) were collected on a Bruker AXS SMART

APEX CCD diffractometer at 100(2) K using monochromatic Mo Kα radiation with omega scan technique. The unit cells were determined using SMART and SAINT+ [16-18], and the data were corrected for absorption using SADABS [17, 18]. The structures were solved by direct methods and refined by full matrix least squares against F^2 with all reflections using SHELXTL [19, 20]. Refinement of an extinction coefficient was found to be insignificant. All non-hydrogen atoms were refined anisotropically. Hydrogen atoms were placed in calculated positions and were refined with an isotropic displacement parameter 1.2 (C-H and CH_2) or 1.5 (CH_3) times that of the adjacent carbon atom. Crystal data and refinement details are listed in Tables 2-6.

2.4. Molecular calculations

Ab initio and semi-empirical calculations were performed using the SPARTAN `04 program (Wave function Inc. 18401 Von Karman Avenue, Suite 370 Irvine, CA92612). Geometry optimizations of initial structures were done using semi-empirical AM1 minimization *in vacuo* to give a reasonable starting geometry for the Hartree-Fock calculations. All *ab initio* minimizations were done using Hartree-Fock calculations with 6-31G* basis set, and density functional theory (DFT) theory calculations were conducted using the B3LYP functional and a 6-31G* basis sets.

3. Results and Discussion

3.1. Spectroscopic Analysis

^{1}H-NMR signals observed were used to identify compound **11** and suggest the structure that was confirmed by X-ray crystallographic data from this study. Compounds

4, **5** and **6** have been previously synthesized and characterized by means of NMR spectroscopy [10, 13, 21]. However, the crystal structure for **5** and **6** had never been reported. For the novel compound (**11**), signals for both the 'bridge' hydrogens (H-7a, 7b) were observed at δ_H 1.34 and δ_H 1.16 ppm. The multiplet observed at 1.47 – 2.00 ppm that integrated for eight protons was assigned to H-4a, 4b, 5a, 5b, 9a, 9b, 10a, 10b. The multiplet observed at 2.35 – 2.62 ppm that integrated for two protons was assigned to H-6 and H-8. The multiplet observed at 2.66 – 2.88 ppm that integrated for two protons was assigned to H-1 and H-2. The quartet at 3.05 – 3.30 ppm that integrated for two protons was assigned to H-3 and H-11. The singlet at 3.57 – 3.69 ppm that integrated for two protons was assigned to H-12a and H-12b and the three protons of the methoxy OCH_3-19 correspond to the singlet at 3.74 – 3.93 ppm. We observed a doublet of doublets at 6.58 – 6.80 ppm that integrated for one proton and we assigned this to H-16. At 6.82 – 6.95 ppm we observed a multiplet that integrated for two protons and we assigned this to H-14 and H-18. The triplet at 7.06 – 7.23 ppm that integrated for one proton was assigned to H-17. The ^{13}C-NMR data are presented in Table 1 and show 14 resonances. The data obtained from the spectroscopic analysis in this study are in full agreement with the X-ray structure.

3.2. X-ray Analysis

One important aspect in molecular recognition is shape. Overall size (i.e. volume) and general geometry (e.g. the x-y-z aspect ratio of a molecule) play crucial roles as to whether a molecule is recognized by a receptor, an active site of a protein, or other shape driven interactions of a small compound with biological macromolecules. For

interactions of molecules with membrane ion channels, size, surface area, and geometrical conformation are of particular importance and it is these properties that determine the activity of a molecule. For polycyclic compounds, for example, the L-type calcium channel blocking activity depends at least partially on the size and geometry of the polycyclic scaffold [6]. Malan *et al*., (2000) determined that changes in the polycyclic structure had a definitive effect on calcium channel blocking activity and that increased inhibition of the calcium current was observed for structures in which the polycyclic 'cages' were enlarged. In this study we determined the single crystal structures of the two triquinane scaffolds (**5** and **6**) and of the substituted derivative (**11**). This allowed us to evaluate geometric feature such as the molecular size and shape. The ORTEP plots in Figures 1(a) and 2(a) give perspective views of tricyclo[6.3.0.$0^{2,6}$]undecane-4,9-diene-3,11-dione (**5**) and tricyclo[6.3.0.$0^{2,6}$]undecane-3,11-dione (**6**). The crystal packing for the two compounds is represented in Figure 1(b & c) and 2(b, c & d). The *cis-syn-cis* linear configuration for both **5** and **6** are clearly visible in the ORTEP plots. This is a unique feature for these compounds as this configuration can only be obtained through thermal fragmentation of the cage structure **4**. Any other approach towards linearly fused triquinanes would result in the *cis-trans-cis* tricyclopentanoid framework [22]. For compound **5** the double bonds between C2 and C3 as well as C7 and C8 provide rigidity to the structure and its framework does not have much flexibility as can also be seen in the crystal packing. Compound **6** lacks the double bonds between C2 and C3 as well as C7 and C8, and this allows for somewhat enhanced flexibility. When compared to related pentacycloundecane counterparts [14], the two triquinane scaffolds **5** and **6** are both more flexible and are also more asymmetric and less globular than the equivalent tetra or

pentacycloundecanes (Figure 3), with much larger x-y aspect ratios than the pentacyclo(5.4.0.0^{2,6}.0^{3,10}.0^{5,9})undecane-8,11-dione (**4,** CCDC entry code: FOBPAO), or related compounds tetracyclo(6.3.0.0^{4,11}.0^{5,9})undecane-2,7-dione (**12**, CCDC entry code: TOHZUL) or pentacyclo(6.2.1.0^{2,7}.0^{4,10}.0^{5,9})undecane-endo-endo-3,6-diol (**13**, CCDC entry code: XIJPEL). An overlay of these compounds which all feature a $C_{11}O_2$ skeleton is shown in Figure 3b. The triquinanes, **5** (red) and especially **6** (blue) are the by far the most asymmetric molecules and are much wider than the tetra or pentacyclic compounds **4**, **12** and **13**. The largest C···C distances within one molecule, indicative of the length of the molecule, are between 3.620 and 3.682 Å for the tetra and pentacyclic compounds. Compounds (**5** and **6**), on the other hand, feature maximum C···C distances of 4.025 and 5.304 Å, respectively. The width of the molecules (measured as the distance between the center of the two oxygen atoms and the methylene carbon atoms at the opposing end of the molecules), on the other hand, are much more uniform and vary only between 4.661 and 4.158 Å. The smallest value of 4.148 Å is associated with compound (**6**), again emphasizing the distorted elongated shape of this molecule. Contributing factors for this observation are of course the absence of the bridging bonds between the carbon atoms in **5** and **6**, and the associated release of strain. In **5** the presence of the sp_2 hybridized carbon atoms somewhat limits the conformational freedom of the carbon skeleton and this molecule has an appearance not too different from that of the tetra or pentacyclic compounds, but with the molecule expanded along the direction of the now missing C-C bond. As a consequence, triquinane **5**, as well as the tetra or pentacyclic compounds, are mostly pseudo-mirror symmetric. The sp_2 hybridization of the carbon atoms leads to a highly strained *cis-syn-cis* linear configuration not too different from those seen for the

tetra or pentacyclic compounds. In **6**, on the other hand, the substitution of the bridgehead or sp_2 hybridized C atoms by sp_3 hybridized CH_2 groups releases most of this strain despite its *cis-syn-cis* linear configuration. Molecule **6** assumes a conformation distinctively different from and much more asymmetric than that of the other four molecules. It has no approximate local mirror symmetry, and the five membered rings are substantially tilted away from each other. This asymmetry and greater flexibility also affects the crystal packing of **6**. The molecules are capable of enveloping each other as can be seen in Figure 2d. Thus the intrinsic expansion by removal of a covalent bond and associated asymmetry which further expands the molecule in one direction around its girth, result in a larger surface area for compound (**6**). This observation was also made in an article by Liebenberg *et al*., (1996) where the author drew comparison between the solvent accessible surface area (SASA) of the pentacycloundecane and triquinane scaffolds. The triquinane scaffold had a larger molecular volume (552 $Å^3$) and SASA (351 $Å^2$) compared to the molecular volume (498 $Å^3$) and SASA (325 $Å^2$) of the pentacycloundecane scaffold.

The increased flexibility and size (determined by molecular surface area and volume) of **6** and to some extend its derivative **11** might be beneficial when designing compounds that act as ion channel blockers due to better geometric conformational fit within the ion-channel. The ORTEP plot in Figure 4 gives a perspective view of *N*-(3-methoxybenzyl)-3,11-azatricyclo[6.3.0.$0^{2,6}$]undecane (**11**) which is a biologically active derivative of **6**. Its crystal structure confirms the results obtained by NMR spectroscopy for this novel compound. From the crystal structure it is evident that the methoxybenzyl side chain does not substantially fold back onto the triquinane scaffold. This is an

important observation that has an influence on the activity as an L-type calcium channel blocker as it was described for the pentacycloundecylamines that compounds where the side chain was able to fold back onto the scaffold had the lowest activity as L-type calcium channel blockers [6]. Another aspect that can be seen from the structure of **11** is that the introduction of the aza-bridge between the two halves of the molecule resulted in some loss of the strain relieve experienced by compound **6**, despite having ethylene groups rather than double bonded sp_2 carbon atoms in the structure. Molecule **11**, when compared to compound **5**, is again much more rigid and the polycyclic part of the molecule now exhibits again a pseudo-mirror plane (Figure 4). For future synthetic approach the benefit of increased flexibility and size could be retained by introducing the amine side chain without transannular cyclization, therefore not adding the aza- or oxa-bridging bond.

3.3. Cyclization Reaction Mechanism

Although the retro cyclization of (**5**) has been reported [15], we wish to elaborate on the mechanism that has been proposed for the somewhat unusual [$_{\pi}2_s$ + $_{\pi}2_s$] photochemical cycloaddition of this highly strained polycyclic system. In the synthesis of **4**, the *endo* Diels-Alder adduct (**3**) was easily converted into the saturated cage isomer (**4**) by photochemical cycloaddition [13]. The proposed mechanism (Scheme 3) for the conversion can be described as excitation of electrons from the highest filled molecular orbital (HOMO) of the bicycloheptene double bond to the lowest vacant molecular orbitals (LUMO) of the enedionechromophore [13], thus allowing for [$_{\pi}2_s$ + $_{\pi}2_s$]

photochemical cyclization to occur according to the Möbius-Hückeltheory [23] as demonstrated by the DFT calculations in Figure 5.

Thermal cleavage or cycloreversion (Scheme 3) of **4** operates by the diradical mechanism, the reverse of a [$_{\pi}2_{s}$ + $_{\pi}2_{s}$] photochemical cycloaddition [23]. However it should be noted that the product formed (**5b**) does not resemble the precursor (**3**) to the cycloaddition as demonstrated by DFT calculations in Figure 5. This is due to the fact that during the cycloreversion bonds 1, 7 and 2, 6 are cleaved instead of 1, 2 and 6, 7 that formed during the cycloaddition step. The isomer that formed is also stereospecific with a *cis-syn-cis* conformation which is unachievable by any other mechanism [9]. The reversion of (**5**) back to (**4**) reaffirms the *cis-syn-cis* stereostructure which allows the intramolecular [$_{\pi}2_{s}$ + $_{\pi}2_{s}$] cycloaddition [9, 24, 25] to occur.

Explaining the mechanism for the [2+2] cycloaddition and cycloreversion can also be aided by Frontier molecular orbital theory (FMO) which has been shown to be a helpful tool in understanding chemical reactions [26]. The DFT level of theory has been found to give satisfactory results for pericyclic reactions, as well as Diels-Alder reactions [26] and was therefore chosen for the FMO evaluations as shown in this study. Single point energies were calculated using the semi-empirical AM1 module. The HOMO and LUMO were also calculated (Figure 5) using DFT and calculations were conducted using the B3LYP functional and a 6-31G* basis. As can be seen from Figure 5, for the photochemically initiated cycloaddition of **3** to give the cage structure **4**, the [2+2] system can easily form under photochemical conditions, to ensure phase alignment of the HOMO-LUMO orbitals. Similarly, DFT calculations also show how the retro-cycloaddition of **5b** back to **4** is possible, as the energy in the form of UV light is

able to phase align the HOMO-LUMO orbitals for sufficient overlap to form a bond. From the calculations, it can be seen that **3** is more likely to undergo cyclization with UV light, as opposed to **5b**, since less phase alignment is needed with **3** than **5b**.

4. Conclusions

Here we presented crystal structure data and explored some of the structural features for two triquinane scaffolds (**5** and **6**) that are structurally related to the pentacycloundecane scaffold (**4**) and useful in the design of multifunctional neuroprotective drugs with activity on both the NMDA receptor channel and the L-type calcium channel. Least squares overlays the two triquinane scaffolds (**5** and **6**) with the tetra (**12**) and pentacycloundecane (**4** and **13**) allowed valuable insight into the differences in size and geometric constrains, which are key features for L-type calcium channel activity of these compounds. We found that substitution of the bridgehead or sp_2 hybridized C atoms by sp_3 hybridized CH_2 groups in triquinane **6** caused strain release, affecting the geometry of the compound, and resulting in an asymmetric compound with greater flexibility and larger surface are. These features enhance the activity of these compounds as L-type calcium channel blockers. We were also able to obtain crystal structure data for **11**, a biological active derivative of **6**, which has activity as an L-type calcium channel blocker. It was observed that the introduction of the aza-bridge in this compound resulted in some loss of the flexibility gained for its precursor, compound **6**. Compound **11** have a calculated log *P* value of 3.51 ± 0.39 (ACD log *P*® software), suggesting a more lipophilic compound with a favorable, although not optimal, blood-brain barrier permeability [1]. Activity for these compounds as L-type calcium channel blockers is

dominated by the lipophilic amine substituent. The triquinane scaffold, in addition to contributing a larger surface area to the geometric conformation, are also a lipophilic carrier with the ability to enhance the compound's pharmacokinetic/pharmacodynamic properties to a favorable distribution in the central nervous system (CNS) [3]. These features are of great benefit when designing drugs for treatment of neurodegenerative disorders. We also explored the photocyclization and cycloreversion reaction mechanisms and computational studies indicate that the cyclization of **3** to **4** is more likely than from **5b** to **4** due to higher activation energy and more suitable phase alignment of the orbitals.

Supplementary crystallographic data for this paper are available from the Cambridge Crystallographic Data Centre (CCDC) electronic archives (Reference: 894408 – 894410). This data can be obtained free of charge from the CCDC via http://www.ccdc.cam.ac.uk/conts/retrieving.html (or from the Cambridge Crystallographic Data Centre, 12, Union Road, Cambridge CB2 1EZ, UK; fax: +44 1223 336033).

Acknowledgments: The X-ray diffractometer was funded by NSF Grant 0087210, Ohio Board of Regents Grant CAP-491, and by Youngstown State University.

References

[1] J. Zah, G. Terre' Blanche, E. Erasmus and S. F. Malan, *Bioorg. Med. Chem.* **2003**, *11*: 3569-3579.

[2] W. J. Geldenhuys, S. F. Malan, J. R. Bloomquist, A. P. Marchand and C. J. Van der Schyf, *Med. Res. Rev.* **2005**, *25*: 21-48.

[3] J. Joubert, W. J. Geldenhuys, C. J. Van der Schyf, D. W. Oliver, H. G. Kruger, T. Govender and S. F. Malan, *Chem. Med. Chem.* **2012**, *7*: 375-384.

[4] W. J. Geldenhuys, M. B. H. Youdim, R. T. Carroll and C. J. Van der Schyf, *Prog. Neurobiol.* **2011**, *94*: 347-359.

[5] C. J. Van der Schyf, G. J. Squier and W. A. Coetzee, *Pharmacol. Res. Comm.* **1986**, *18*: 407-417.

[6] S. F. Malan, J. J. Van der Walt and C. J. Van der Schyf, *Arch. Pharm. (Weinheim).* **2000**, *333*: 10-16.

[7] C. Kiewert, J. Hartmann, J. Stoll, T. J. Thekkumkara, C. J. Van der Schyf and J. Klein, *Neurochem. Res.* **2006**, *31*: 395-399.

[8] W. J. Geldenhuys, S. F. Malan, J. R. Bloomquist and C. J. Van der Schyf, *Bioorg. Med. Chem.* **2007**, *15*: 1525-1532.

[9] G. Mehta, A. Srikrishna, A. V. Reddy and M. S. Nair, *Tetrahedron.* **1981**, *37*: 4543-4559.

[10] W. Liebenberg, P. H. Van Rooyen and C. J. Van der Schyf, *Pharmazie.* **1996**, *51*: 20-24.

[11] T. Yagami, K. Ueda, T. Sakaeda, N. Itoh, G. Sakaguchi, N. Okamura, Y. Hori and M. Fujimoto, *Biochem. Pharmacol.* **2004**, *67*: 1153-1165.

[12] T. Kobayashi and Y. Mori, *Eur. J. Pharmacol.* **1998**, *363*: 1-15.

[13] R. C. Cooksen, E. Grundwell and J. Hudec, *Chem. Ind.* **1958**, 1004-1003.

[14] A. Linden, J. Romanski, G. Mloston and H. Heimgartner, *Acta Crystallogr. C.* **2005**, *C61*: o221-o226.

[15] G. Mehta, D. S. Reddy and A. V. Reddy, *Tetrahedron Lett.* **1984**, *25*: 2275-2278.

[16] *Bruker Advanced X-ray Solutions SMART for WNT/2000 (Version 5.628), Bruker AXS Inc., Madison, Wisconsin: USA.* ***1997-2002***.

[17] *Bruker Advanced X-ray Solutions SAINT (Version 6.45), Bruker AXS Inc., Madison, Wisconsin: USA.* ***1997-2003***.

[18] *Bruker Advanced X-ray Solutions SADABS in SAINT (Version 6.45), Bruker AXS Inc., Madison, Wisconsin: USA.* ***1997-2003***.

[19] *Bruker Advanced X-ray Solutions SHELXTL (Version 6.10), Bruker AXS Inc., Madison, Wisconsin: USA.* ***2000***.

[20] G. M. Shieldrick, *Acta Crystallogr. A.* **2008**, *A64*: 112-122.

[21] G. Mehta and K. S. Rao, *J. Org. Chem.* **1985**, *50*: 5537-5543.

[22] G. Mehta and A. Srikrishna, *Chem. Rev.* **1997**, *97*: 671-720.

[23] M. B. Smith and J. March, *March's advance organic chemistry*, Wiley-Interscience Publication, **2001**, p. 2083.

[24] G. Mehta, A. V. Reddy, A. N. Murthy and D. S. Reddy, *J. Chem. Soc. Chem. Commun.* **1983**, *824*.

[25] G. Mehta and A. V. Reddy, *J. Chem. Soc. Chem. Commun.* **1981**, *756*: 756-757.

[26] M. A. Silva, S. C. Pellegrinet and J. M. Goodman, *J. Org. Chem.* **2003**, *68*: 4059-4066.

Figure 1a

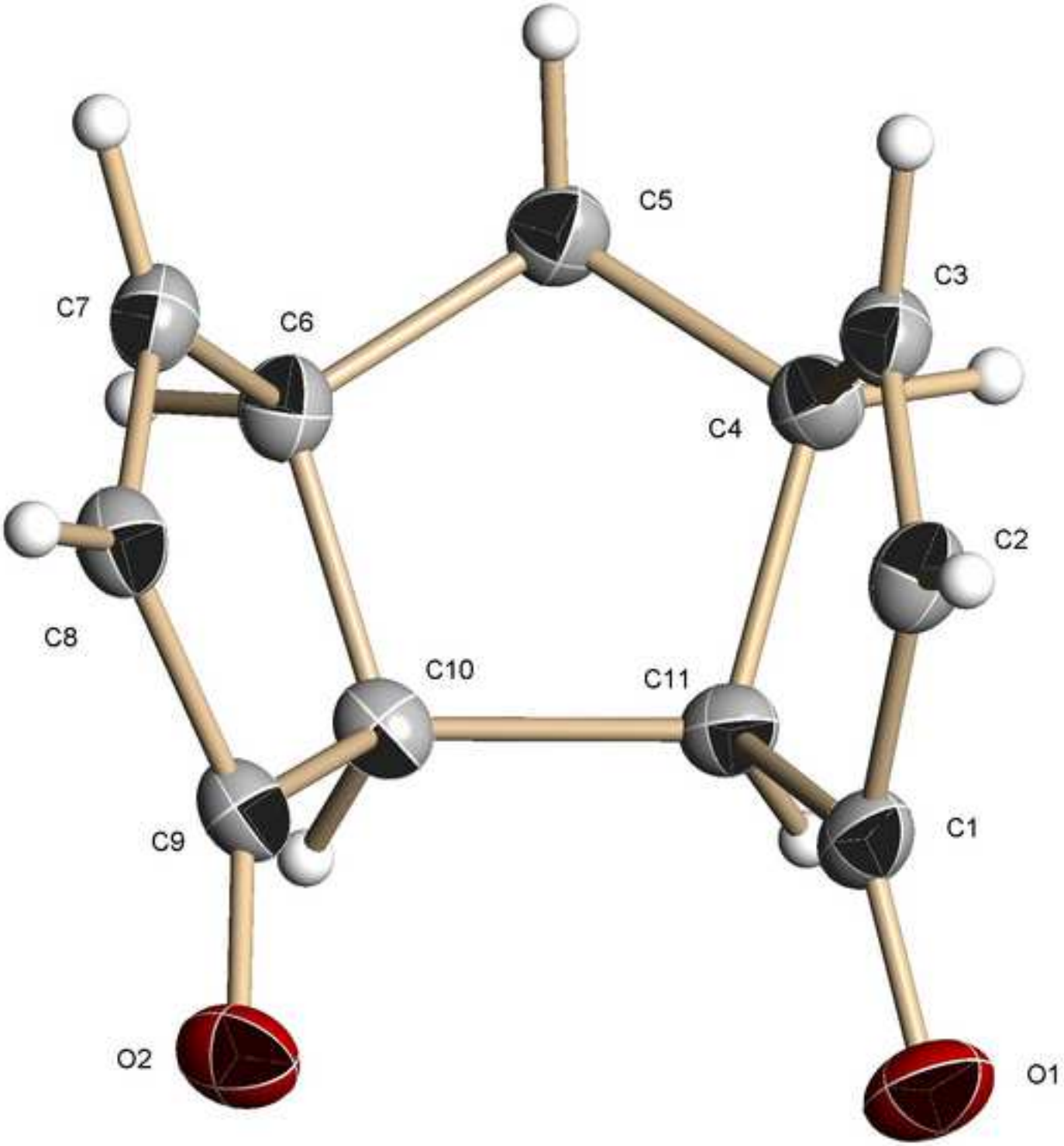

Figure 1b

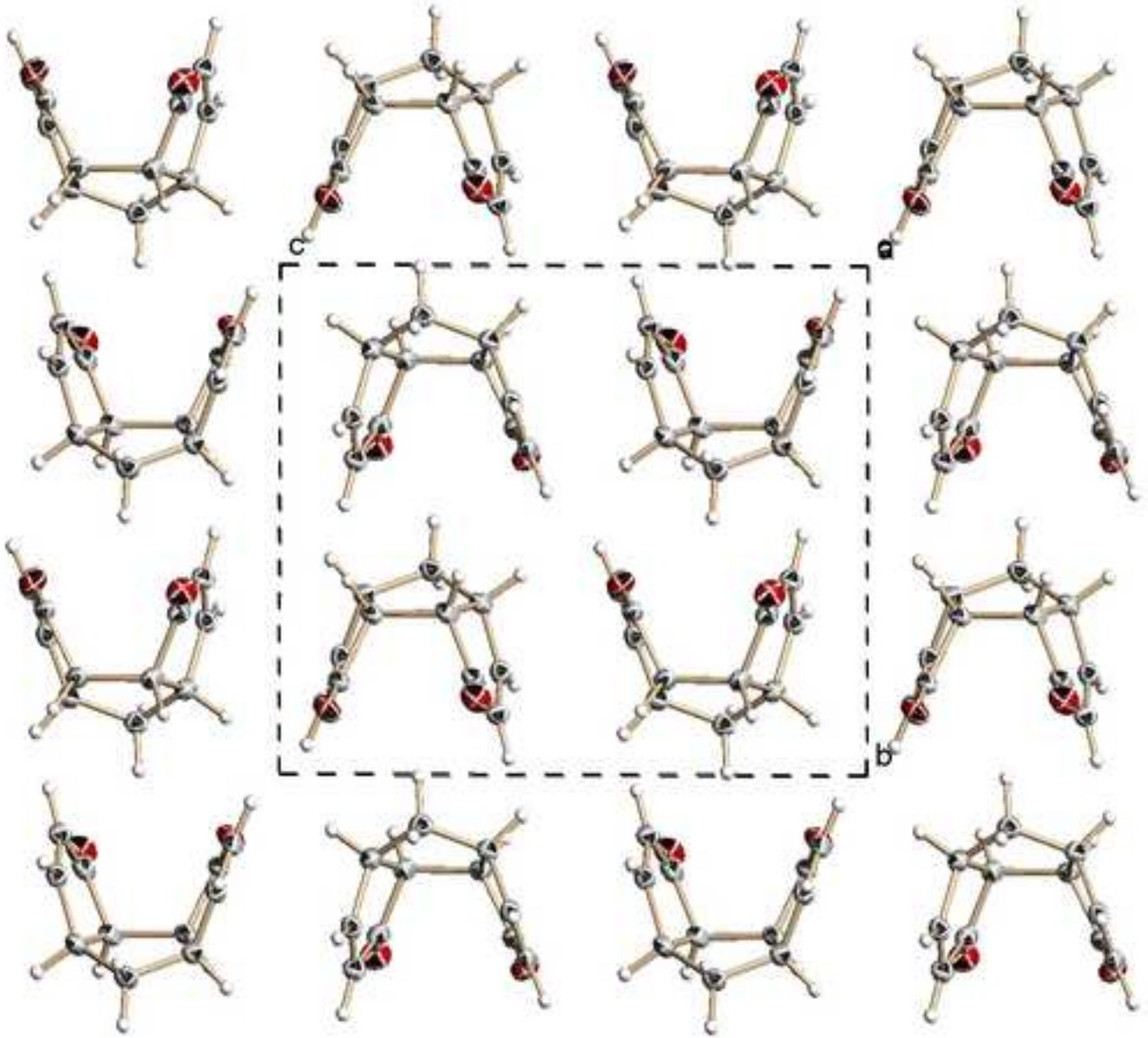

Figure 1c

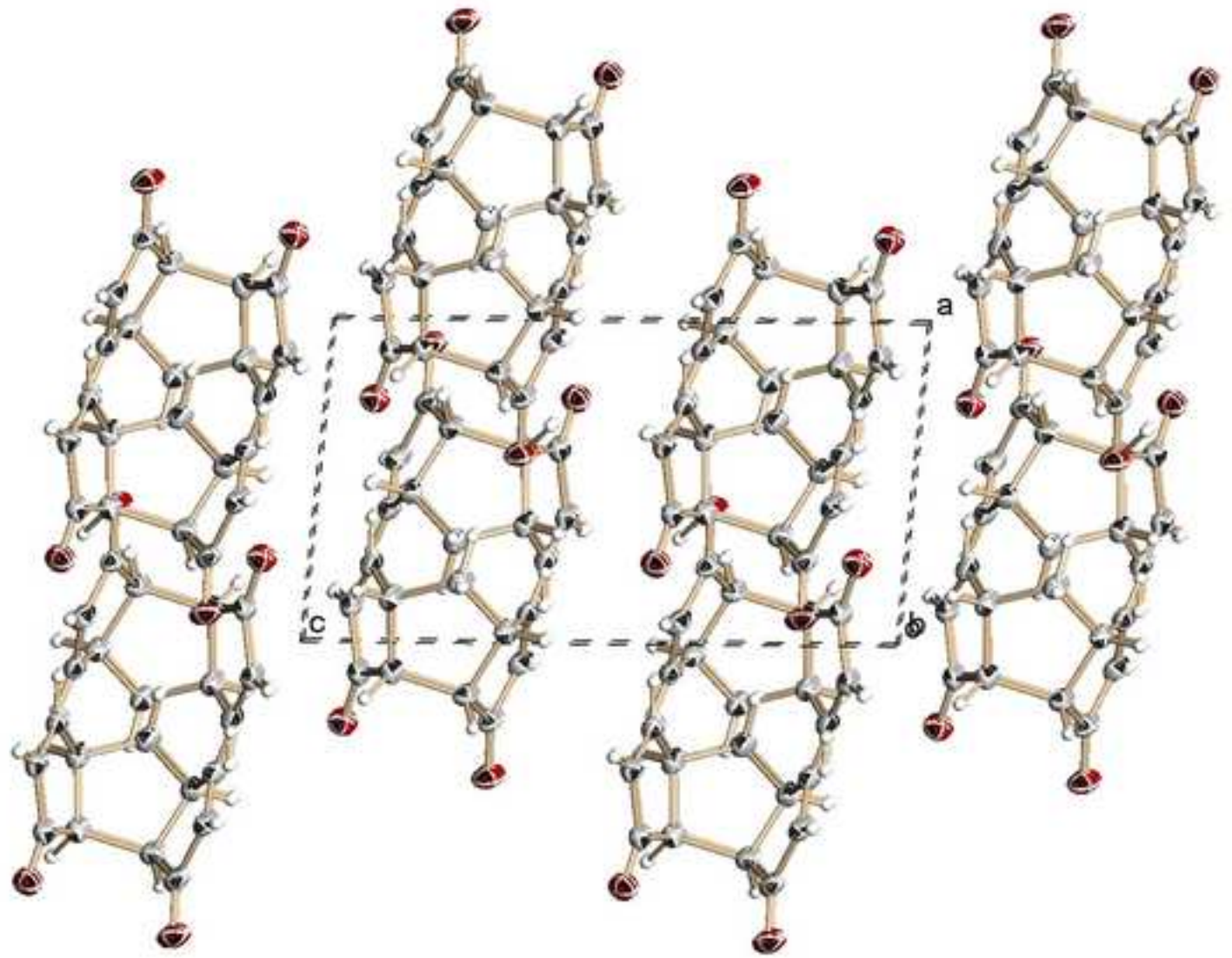

Figure 2a

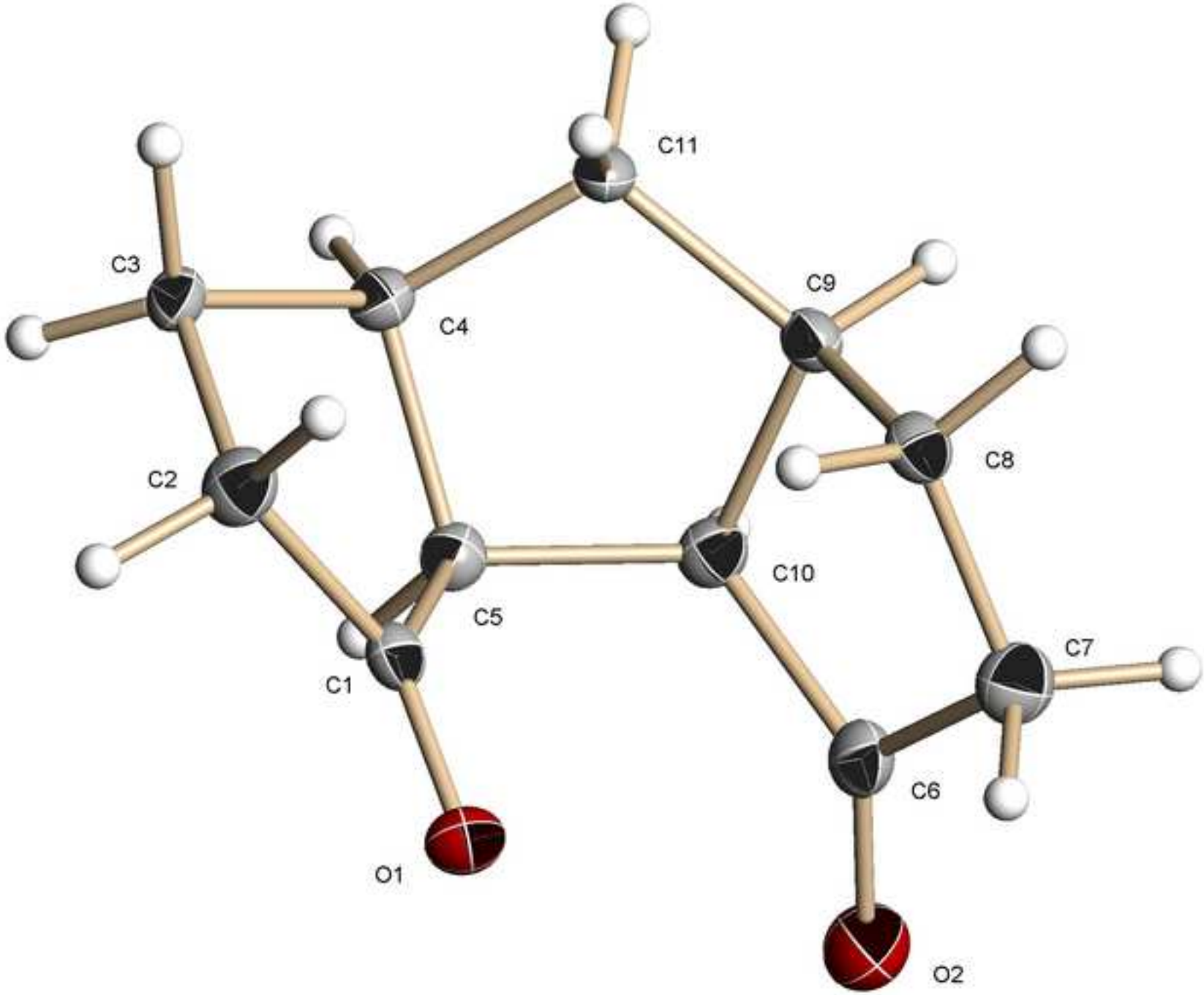

Figure 2b

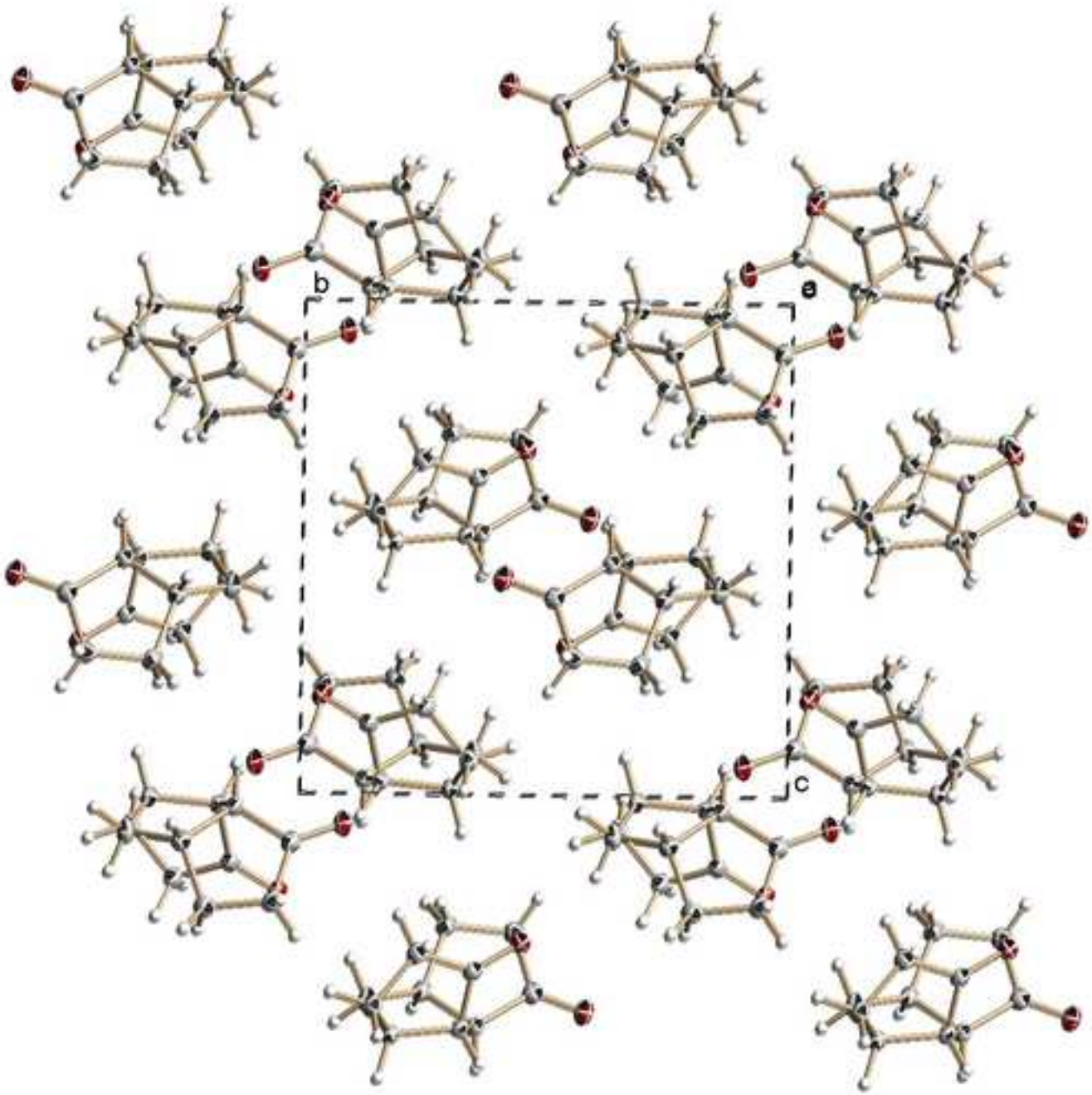

Figure 2c

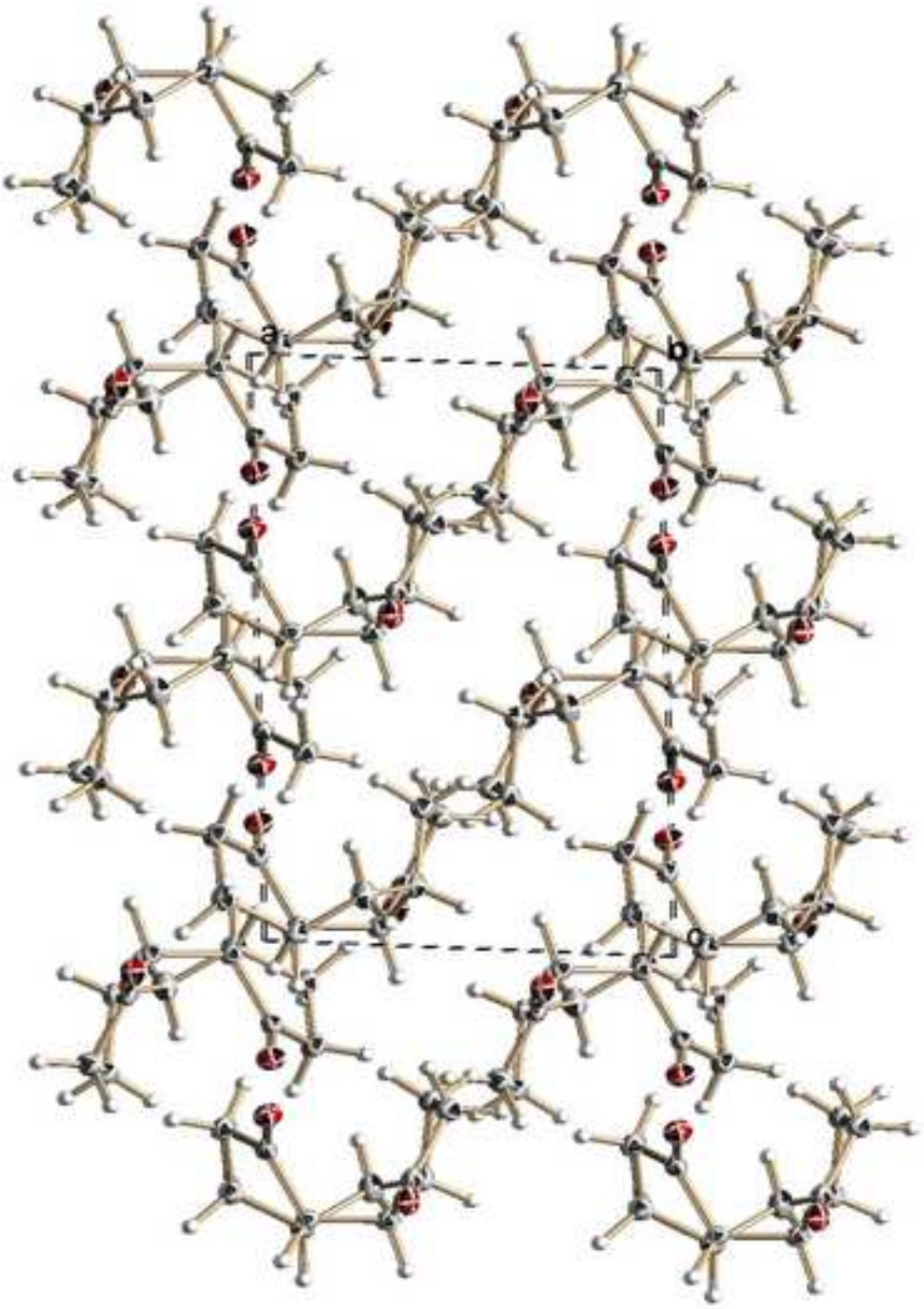

Figure 2d

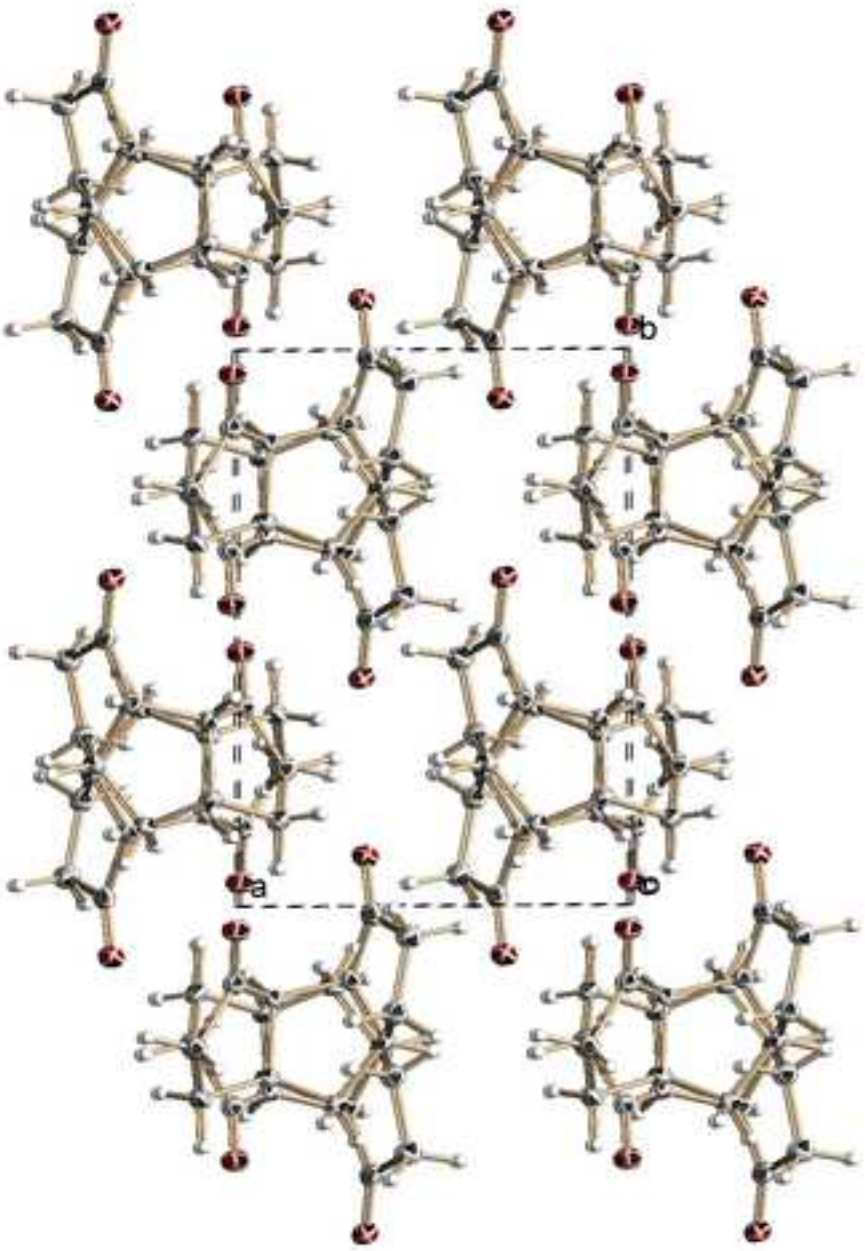

Figure 3a

(4) 

(12) 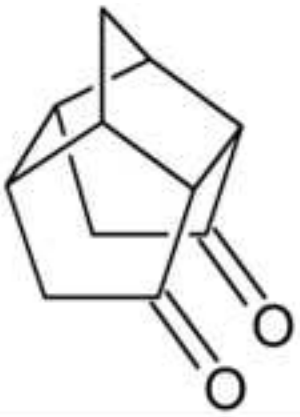

(13) 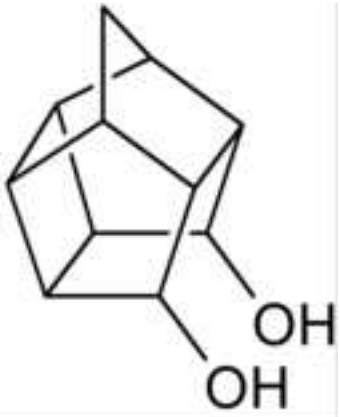

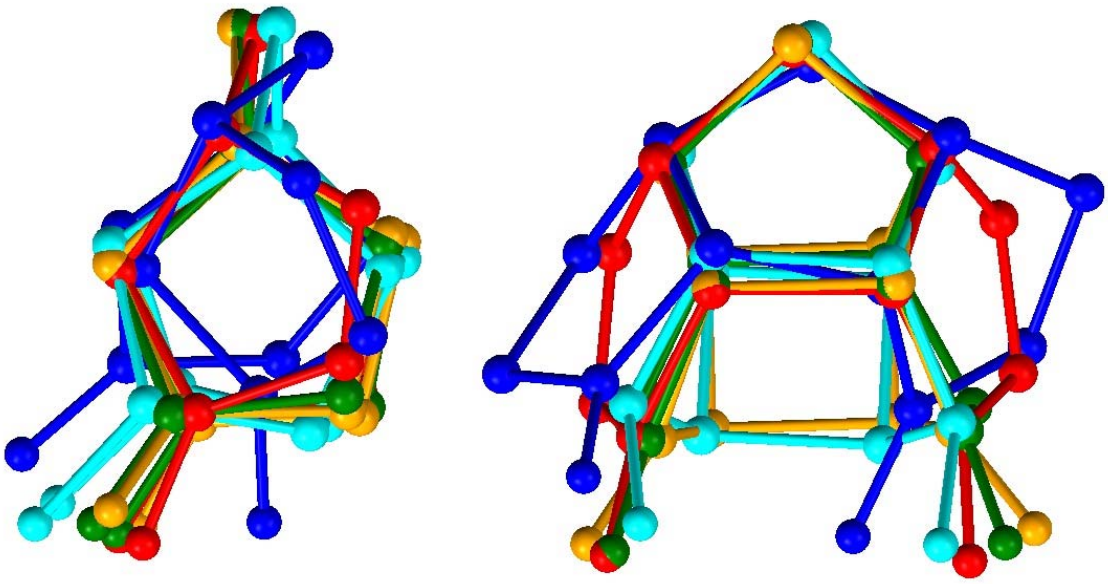

Fig 3b

Figure 4

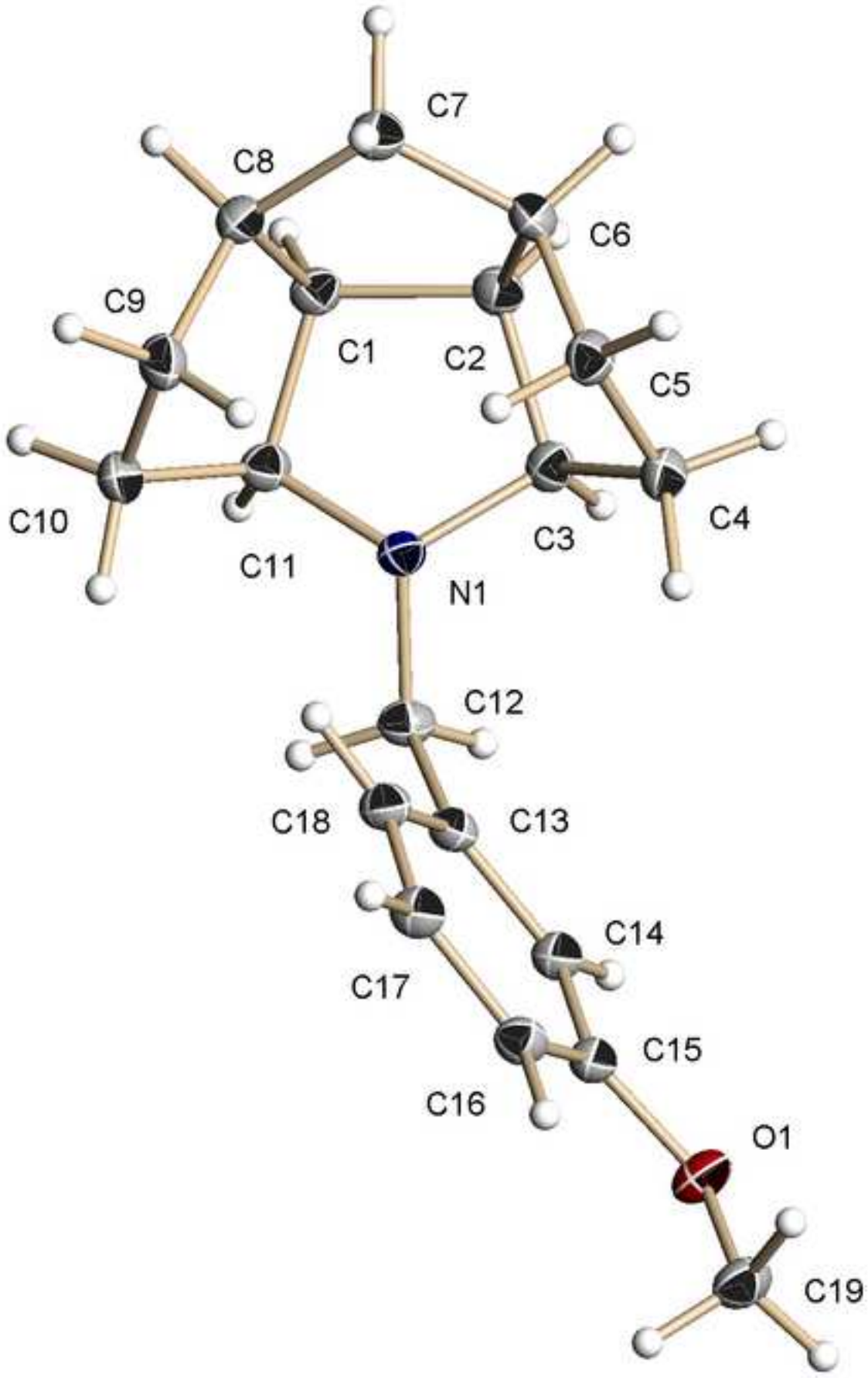

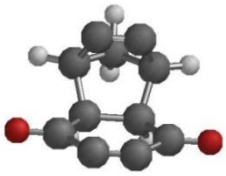	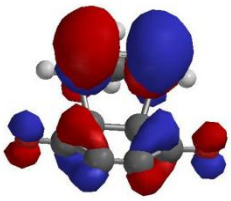	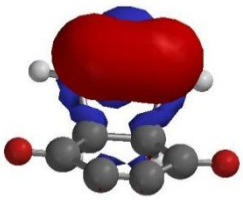
3	**LUMO**	**HOMO**
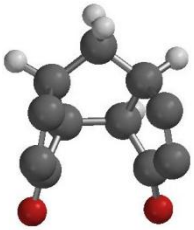	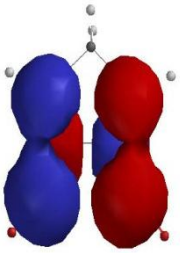	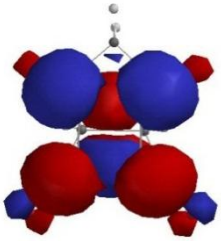
5b	**LUMO**	**HOMO**

Figure 5. Calculated HOMO & LUMO surfaces for compounds **3** and **5b**.

Figure Graphical Abstract

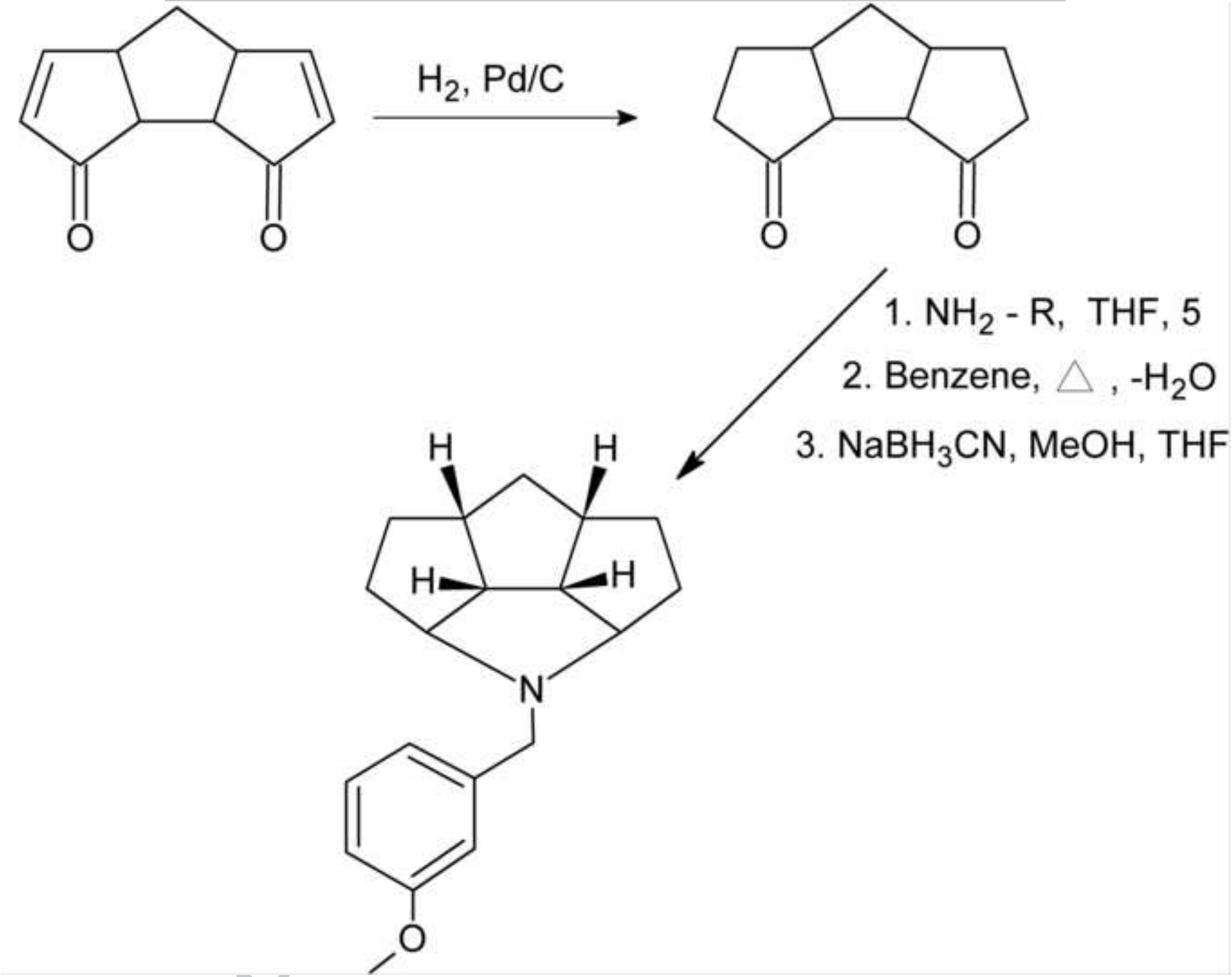

Scheme 1

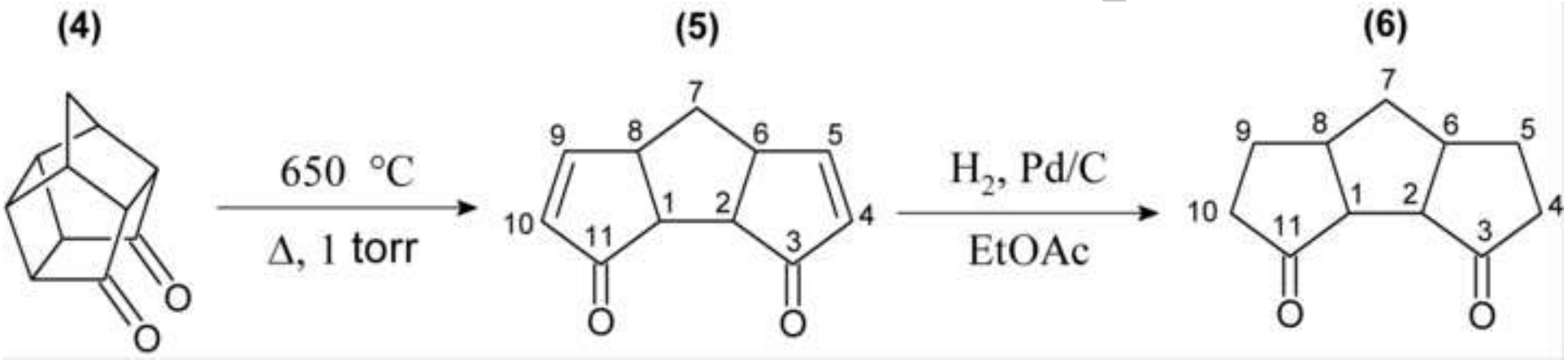

Scheme 2

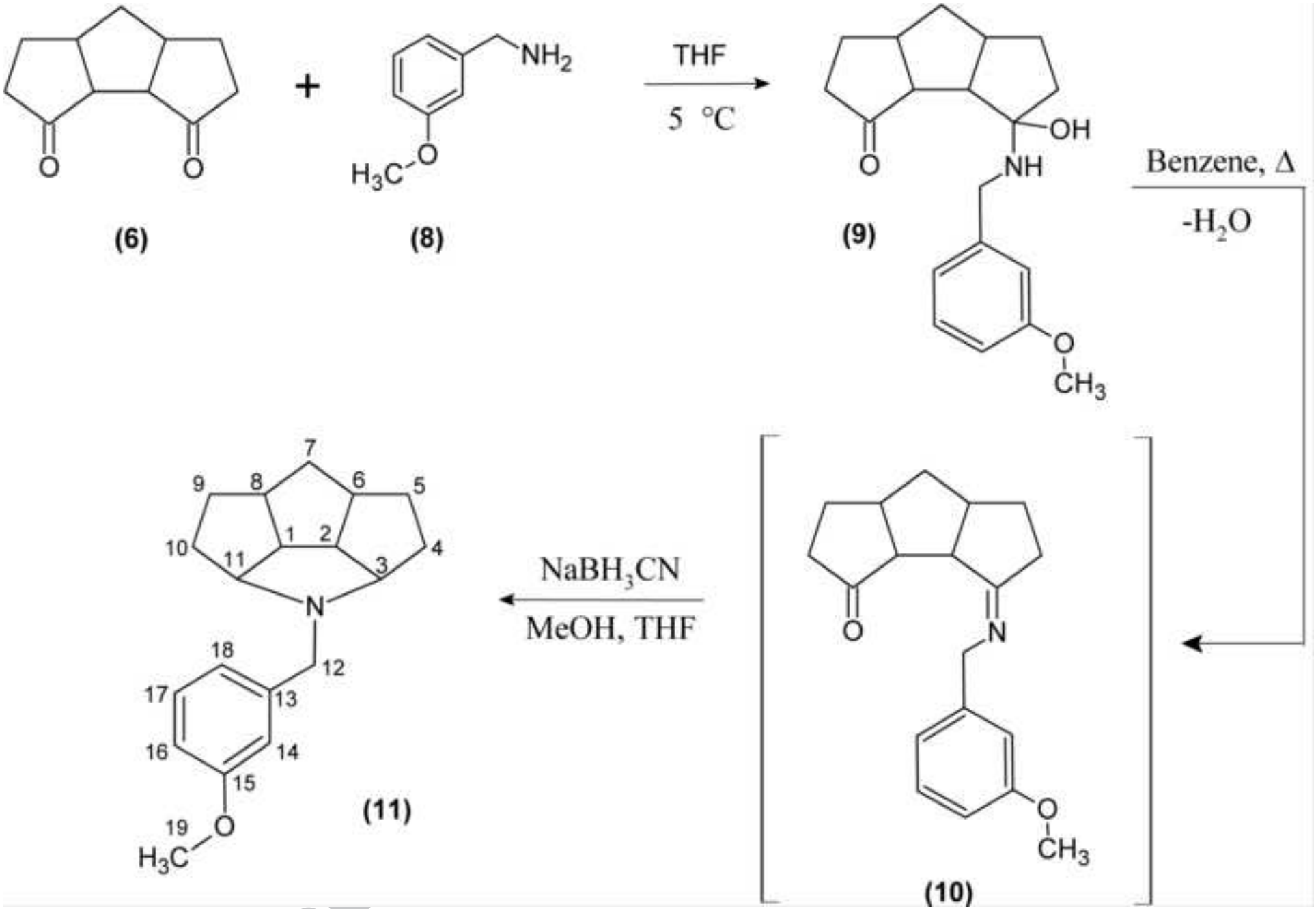

Scheme 3

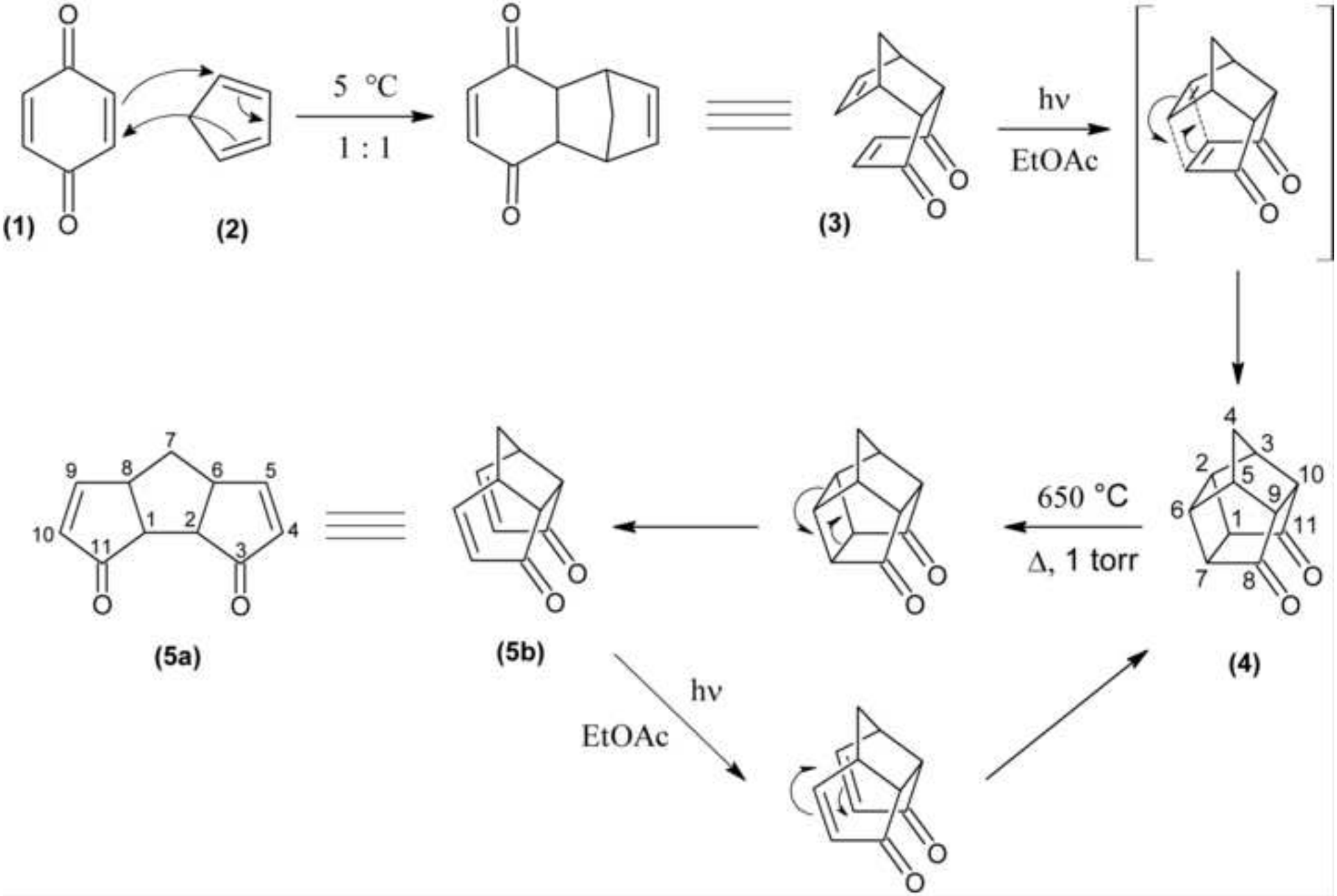

Table 1. ^{13}C-NMR data (δ, ppm) of compound **11**

Carbon atoms	δ_C
C-15	159.38 (s)
C-13	142.99 (s)
C-17	128.75 (d)
C-18	120.92 (d)
C-14	114.05 (d)
C-16	111.93 (d)
C-3, 11	73.73 (d)
C-12	58.56 (t)
C-19	55.10 (q)
C-1, 2	54.49 (d)
C-6, 8	47.34 (d)
C-7	37.45 (t)
C-4, 10	34.51 (t)
C-5, 9	32.79 (t)

Table 2. Crystal data and refinement details for tricyclo[6.3.0.0^{2,6}]undecane-4,9-diene-3,11-dione (**5**) and tricyclo[6.3.0.0^{2,6}]undecane-3,11-dione (**6**)

Compound	**5**	**6**
Chemical formula	$C_{11}H_{10}O_2$	$C_{11}H_{14}O_2$
Formula weight	174.19 g/mol	178.22 g/mol
Crystal shape, colour	Block, colorless	Block, colorless
Crystal size	0.44 × 0.39 × 0.24 mm	0.61 × 0.39 × 0.34 mm

Crystal system	Monoclinic	Monoclinic
Space group	$P2_1/n$	$P2_1/c$
Unit cell dimensions	a = 6.5876 (12) Å	a = 7.5992 (7) Å
	b = 10.4204 (19) Å	b = 10.7294 (10) Å
	c = 12.074 (2) Å	c = 10.8664 (10) Å
	α = 90º	α = 90º
	β = 95.201 (4) º	β = 93.805 (2) º
	γ = 90º	γ = 90º
Volume	825.4 (3) $Å^3$	884.04 (14) $Å^3$
Formula units (Z)	4	4
Density (D*x*, calculated)	1.402 Mg/m^3	1.339 Mg/m^3
μ (MoKα)	0.096 mm^{-1}	0.091 mm^{-1}
F (000)	368	384
Temperature	100 (2) K	100 (2) K
Theta (θ) range for data collection	2.59 – 28.25º	2.67 – 28.28º
Reflections measured	4762	7138
Unique reflections	2013	2168
R_{int}	0.0187	0.0208
Observed data ($I > 2\sigma(I)$)	1754	1949
R_1, wR_2, goodness-of-fit (S)	0.0508, 0.1215, 1.065	0.0477, 0.1229, 1.050
$R[F^2 > 2\sigma(F^2)]$	0.0451	0.0440
$(\Delta/\sigma)_{max}$	0.000	0.000
$\Delta\rho_{min}$, $\Delta\rho_{max}$	-0.212, 0.370 e $Å^{-3}$	-0.195, 0.416 e $Å^{-3}$
T_{min}	0.977	0.970

T_{max}	0.876	0.886
H	-8 → 6	-10 → 10
K	-13 → 13	-14 → 14
L	-15 → 14	-14 → 12
Parameters	118	118

Table 3. Selected geometric parameter (Å, º) for tricyclo[6.3.0.0^{2,6}]undecane-4,9-diene-3,11-dione (**5**)

C1-O1	1.2160 (15)	C6-C7	1.5069 (16)
C1-C2	1.4748 (17)	C6-C10	1.5464 (17)
C1-C11	1.5291 (16)	C7-C8	1.3349 (17)
C2-C3	1.3348 (17)	C8-C9	1.4681 (17)
C3-C4	1.5111 (16)	C9-02	1.2213 (15)
C4-C5	1.5266 (17)	C9-C10	1.5344 (16)
C4-C11	1.5460 (16)	C10-C11	1.5758 (17)
C5-C6	1.5331 (16)		
C2-C3-C4-C11	14.53 (14)	C2-C1-C11-C4	20.67 (12)
C8-C9-C10-C6	-9.27 (12)	C10-C6-C7-C8	-9.70 (14)

Table 4. Selected geometric parameter (Å, º) for tricyclo[6.3.0.0^{2,6}]undecane-3,11-dione (**6**).

C1-O1	1.2143 (14)	C6-O2	1.2119 (14)
C1-C2	1.5169 (15)	C6-C7	1.5205 (16)
C1-C5	1.5260 (15)	C6-C10	1.5237 (15)

C2-C3	1.5303 (16)	C7-C8	1.5319 (16)
C3-C4	1.5380 (15)	C8-C9	1.5485 (16)
C4-C5	1.5415 (15)	C9-C10	1.5430 (15)
C4-C11	1.5544 (15)	C9-C11	1.5477 (15)
C5-C10	1.5400 (14)		
C2-C3-C4-C5	36.26 (11)	C2-C1-C5-C4	14.40 (11)
C8-C9-C10-C6	-27.43 (11)	C10-C6-C7-C8	11.80 (12)

Table 5. Crystal data and refinement details for *N*-(3-methoxybenzyl)-3,11-azatricyclo[6.3.0.0^{2,6}]undecane (**11**)

Chemical formula	$C_{19}H_{25}NO$
Formula weight	283.40 g/mol
Crystal shape, colour	Block, colorless
Crystal size	0.52 × 0.49 × 0.41 mm
Crystal system	Triclinic
Space group	$P\bar{1}$
Unit cell dimensions	a = 7.6714 (7) Å
	b = 9.0100 (9) Å
	c = 11.2539 (11) Å
	α = 103.892 (2) º
	β = 92.749 (2) º
	γ = 97.663 (2) º
Volume	745.78 (12) Å^3

Formula units (Z)	2
Density (D*x*, calculated)	1.262 Mg/m^3
μ (MoKα)	0.077 mm^{-1}
F (000)	308
Temperature	100 (2) K
Theta (θ) range for data collection	1.87 – 28.28º
Reflections measured	7817
Unique reflections	3687
R_{int}	0.0181
Observed data ($I > 2\sigma(I)$)	3265
R_1, wR_2, goodness-of-fit (S)	0.0509, 0.1284, 1.052
$R[F^2 > 2\sigma(F^2)]$	0.0462
$(\Delta/\sigma)_{max}$	0.000
$\Delta\rho_{min}$, $\Delta\rho_{max}$	-0.210, 0.396 e $Å^{-3}$
T_{min}	0.969
T_{max}	0.925
H	-10 → 10
K	-12 → 12
L	-14 → 14
Parameters	265

Table 6. Selected geometric parameter (Å, º) for *N*-(3-methoxybenzyl)-3,11-azatricyclo[6.3.0.$0^{2,6}$]undecane (**11**).

N1-C3	1.4690 (14)	O1-C15	1.3711 (13)
N1-C11	1.4722 (13)	O1-C19	1.4279 (13)

N1-C12	1.4588 (13)		
C13-C12-N1-C3	92.88 (11)	C14-C15-O1-C19	178.94 (9)
N1-C12-C13-C18	44.95 (14)	C16-C15-O1-C19	-0.14 (16)
C13-C12-N1-C11	-138.38 (10)		

Graphical Abstract

Triquinane scaffolds: Shape and geometry as a function of saturation and bridgehead groups.

Lois-May Young,[a] Matthias Zeller,[b] Werner J. Geldenhuys,[c] Sarel F. Malan,[d] and Cornelis J. Van der Schyf[a,c*]

[a]Pharmaceutical Chemistry, School of Pharmacy, North-West University, Potchefstroom 2520, South Africa, [b]Department of Chemistry, Youngstown State University, Youngstown, Ohio 44555, USA, [c]Department of Pharmaceutical Sciences, Northeast Ohio Medical University, Rootstown, Ohio 44272, USA, [d]School of Pharmacy, University of the Western Cape, Bellville, 7535, South Africa

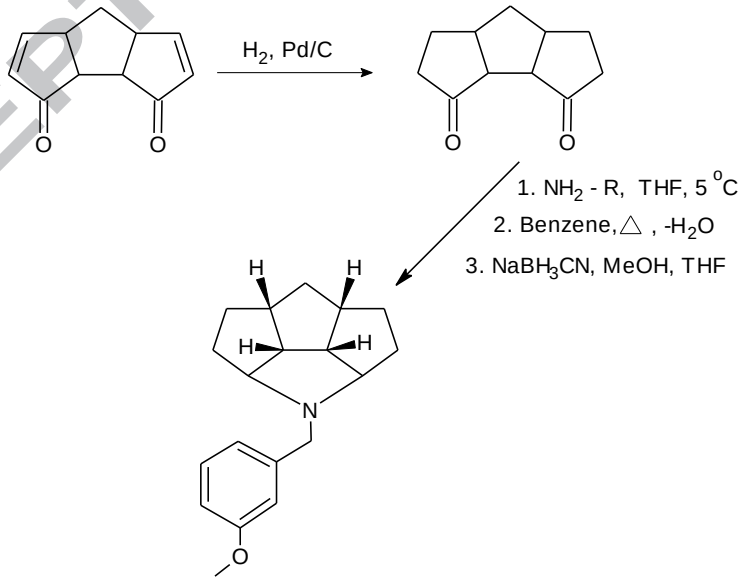

Triquinane scaffolds: Shape and geometry as a function of saturation and bridgehead groups.

Lois-May Young,[a] Matthias Zeller,[b] Werner J. Geldenhuys,[c] Sarel F. Malan,[d] and Cornelis J. Van der Schyf[a,c*]

[a]*Pharmaceutical Chemistry, School of Pharmacy, North-West University, Potchefstroom 2520, South Africa,* [b]*Department of Chemistry, Youngstown State University, Youngstown, Ohio 44555, USA,* [c]*Department of Pharmaceutical Sciences, Northeast Ohio Medical University, Rootstown, Ohio 44272, USA,* [d]*School of Pharmacy, University of the Western Cape, Bellville, 7535, South Africa*

Highlights

- Synthesis of triquinane and triquinylamine derivatives
- Characterization of compounds by means of single crystal X-ray analysis.
- Geometry as a function of saturation and bridgehead groups are discussed.
- Photocyclization and cycloreversion reaction mechanisms are explored.

Captions

Table 1. ^{13}C-NMR data (δ, ppm) of compound **11**

Table 2. Tricyclo[6.3.0.0^{2,6}]undecane-4,9-diene-3,11-dione (**5**) and tricyclo[6.3.0.0^{2,6}]undecane-3,11-dione (**6**)

Table 3. Selected geometric parameter (Å, º) for tricyclo[6.3.0.0^{2,6}]undecane-4,9-diene-3,11-dione (**5**)

Table 4. Selected geometric parameter (Å, º) for tricyclo[6.3.0.0^{2,6}]undecane-3,11-dione (**6**).

Table 5. Crystal data and refinement details for *N*-(3-methoxybenzyl)-3,11-azatricyclo[6.3.0.0^{2,6}]undecane (**11**)

Table 6. Selected geometric parameter (Å, º) for *N*-(3-methoxybenzyl)-3,11-azatricyclo[6.3.0.0^{2,6}]undecane (**11**).

Scheme 1. The synthesis route to obtain tricyclo[6.3.0.0^{2,6}]undecane-4,9-diene-3,11-dione (**5**) and tricyclo[6.3.0.0^{2,6}]undecane-3,11-dione (**6**).

Scheme 2. The synthesis route to obtain *N*-(3-methoxybenzyl)-3,11-azatricyclo[6.3.0.0^{2,6}]undecane (**11**).

Scheme 3. Diels-Alder reaction yielding the Diels-Adler adduct (**3**) followed by UV-initiated photochemical cyclization to yield Cookson's cage compound (**4**). Thermal fragmentation of the pentacyclo[5.4.0.$0^{2,6}$.$0^{3,10}$.$0^{5,9}$]undecane-8,11-dione (**4**) to yield the tricyclo[6.3.0.$0^{2,6}$]undecane-4,9-diene-3,11-dione (**5**) and the reversion back to **4**.

Figure 1. The molecular conformation (a) of tricyclo[6.3.0.$0^{2,6}$]undecane-4,9-diene-3,11-dione (**5**), showing the atomic numbering scheme and displacement ellipsoids at the 50% probability level as well as the crystal packing (b) and (c).

Figure 2. The molecular conformation (a) of tricyclo[6.3.0.$0^{2,6}$]undecane-3,11-dione (**6**), showing the atomic numbering scheme and displacement ellipsoids at the 50% probability level as well as the crystal packing (b), (c) and (d).

Figure 3. Overlay of the tetracycloundecane **12** and pentacycloundecanes **4** and **13,** as well as the two triquinanes **5** and **6**. Colour coding: (**4**) yellow, (**12**) green, (**13**) turquoise, (**5**) red and (**6**) blue.

Figure 4. The molecular conformation of *N*-(3-methoxybenzyl)-3,11-azatricyclo[6.3.0.$0^{2,6}$]undecane (**11**), showing the atomic numbering scheme and displacement ellipsoids at the 50% probability level

Figure 5. Calculated HOMO & LUMO surfaces for compounds **3** and **5b**.